Roger H.L. Chen
Dept. of Civ. and Envir. Engrg.
West Virginia University
Morgantown, WV 26506.
hlchen@wvu.edu
Telephone: 304-293-3031x.2631
Fax: 304-293-7109

Alejandro C. Kiriakidis L
Dept. of Civ. and Envir. Engrg.
West Virginia University
Morgantown, WV 26506.
akiriaki@wvu.edu
Telephone: 304-293-3031x.2434
Fax: 304-293-7109

Nondestructive Evaluation of Stiffness and Stresses of Ceramic Candle Filters at Elevated Temperature under Vibrational Environment

Keywords: Nondestructive Evaluation, Ceramic Candle Filters, Vibration Stresses, Finite Element Analysis.

Introduction

In recent years a significant amount of effort has been devoted to develop damage-tolerant hot gas filter elements, which can withstand chemical, high pressure and extreme thermal cyclic loading in the coal-based environment (Alvin 1999, Spain and Starrett 1999). Ceramic candle filters have proven to be an effective filter for the ash laden gas streams, protecting the gas turbine components from exposure to particulate matter (Lippert et al. 1994). Ceramic candle filters need to sustain extreme thermal environment and vibration-induced stresses over a great period of time. Destructive tests have been used to describe physical, mechanical and thermal properties of the filters and to relate these properties and behaviors to in-service performance, and ultimately to predict the useful life of the filter materials (Pontius and Starrett 1994, Alvin et al. 1994). Nondestructive evaluation (NDE) techniques have been developed to determine the deterioration or the presence of damage and to estimate the remaining stiffness of ceramic candle filters (Chen and Kiriakidis 2001).

This paper presents a study of parameters involved in the prediction of remaining life of ceramic candle filters under service conditions. About one hundred ceramic candle filters from previous studies (Chen and Kiriakidis 2000) and forty-six filters received during this project have been nondestructively evaluated. They are divided in Pall Vitropore, Schumacher and Coors filters. Forty-six of these filters were used having various in-service exposure times at the PSDF and the rest were unused filters. Dynamic characterization tests were employed to investigate the material properties of ceramic candle filters. The vibration frequency changes due to exposure hours, dust cake accumulation, candle's axisymmetry, boundary conditions and elevated temperatures are studied. Investigations on fatigue stresses of the filters due to vibration of the plenum and back pulse shaking are also studied. Finite element models (FEM) are built to calculate the filter's dynamic response with different boundary conditions at various temperatures. The experimental natural frequencies of the candle filters were also compared with an analysis of a general Timoshenko beam equation that includes various boundary restraints.

Objectives

The objectives of this study are to develop an effective nondestructive evaluation (NDE) technique to predict the remaining useful life of ceramic candle filters and to implement the NDE technique for industrial application. Material property degradation of ceramic candle filters are evaluated as a function of exposure time to advanced fossil fuel power generation systems. This is accomplished through analysis of natural frequency vibration signatures of candle filter elements exposed at the DOE Power System Development Facility (PSDF). This study also investigates various factors involved in establishment of an in-situ, routine inspection of ceramic candle filters during routine power plants outages.

Approach

The methodology used in this project is focused on the development of NDE technique based on dynamic characterization. Hammer-impact vibration tests are conducted on each candle filter specimen at different locations. Contact and non-contact sensors are used to measure the vibration response of the filter. This technique is used to evaluate the relationship between changes in the vibration frequencies and remaining life of the ceramic candle filters. The vibration frequency changes due to different factors that are presented during regular power plant operational conditions are studied. FEM are built for each specimen type to understand its dynamic response and its results are compared with the NDE test results. FEM transient thermal analysis models are also built to simulate time dependent heat transfer that occurs during back pulse cleaning. Investigations on fatigue stresses of the filters due to vibration of the plenum and back pulse shaking are conducted using cyclic fatigue tests.

Project description

This project is being conducted under DOE/NETL support, under the contract DE-FG26-99FT40202. New and used ceramic candle filters from various manufacturers are used to study the relationship between the natural frequency and the candle filter's stiffness. The tasks including in this project are: task 1 - data synthesis and evaluation of the candle filters and task 2 - analysis of the results from task 1 using a combination of FEM simulations and theoretical equations.

In task 1, the parameters for assessing deterioration of the candle filter elements from various manufactures are established based on natural frequencies shift and mode shape analysis. The effects of dust cake, boundary conditions, axes of symmetry, elevated temperatures and plenum and back pulse vibration on the vibration response of the candle filters are investigated.

In task 2, analyses are conducted using FEM, strain energy theory, and beam vibration theory. An evaluation method to establish a filter element's damage condition, to understand the cause of a filter failure, and to understand the causes of stiffness degradation is developed. Parametric studies using FEM models are conducted to understand the influence of material properties on vibration response. Analytical equations are studied for the development of an empirical equation for Young's modulus calculation. The results of the analytical expression are compared with FEM and experimental results to validate this approach. The minimum stiffness needed for the filter survival is estimated, and the method to predict filter element useful life is developed during this task.

Results

The deterioration of all the ceramic candle filter specimens due to different exposure hours is summarized in Figure 1. This figure shows the average Young's modulus values of the filters in each filter group at different used hours. The three groups of candle filter from Pall, Schumacher and Coors can be clearly seen. After a few hundred hours of exposure, the Pall and Coors filters groups deteriorate in a linear pattern. The maximum stiffness reduction of a Pall 326-# and a Pall 442T filter, after 3200 exposure hours is about 8.7% and 10.5%, respectively, while the averaged deterioration of four Pall 326-A at 1300 hr is about 5.3%. The stiffness reduction of filters Sch TF-20 an exponential curve pattern while the Sch F40 follows a linear deterioration pattern. For two Sch TF-20 324 filters used for more than 2600hr, the stiffness deterioration is about 10.5%, while for seven Sch F40 (~1860hr) and one Sch TF-20 379H (~1350hr) the average stiffness decreased about 8.4% and 17.1%, respectively. Finally, the maximum averaged stiffness reduction for two Coors P100A filters after 622hr is about 5.5%. The values shown in this figure are averaged results, it has been reported (Chen and Kiriakidis 2001) that the stiffness reduction for individual filter specimens is quite different. Each candle filter has its own distinct behavior, and the stiffness deterioration of each filter can be traced individually using the nondestructive technique.

After been used for a period of time, candle filters present ash accumulation. In order to determine its influence on the dynamic behavior of the candle filters, 12 candle filters were tested before and after cleaning with water. Although dust-cake does not produce any significant change of the specimen's weight (<1% change), the vibration frequency values are always higher for the filters before cleaning than after cleaning. The percentage difference of vibration frequencies between clean and unclean varies. Such anomalies in results are possible due to the formation of temporary, stiffer particulate layers on the walls of the ceramic candle filters.

The percentage differences of natural frequencies between two perpendicular directions for all candle filters with free-free boundary condition were obtained. The difference in natural frequencies between the two axes is generally very small (less than 1%). Some ceramic candle filters have identical frequency values in the two perpendicular axes. The axisymmetric behavior of candle filters was also obtained when fixed-free boundary condition was imposed.

The relationships between the frequency values, Young's modulus and boundary restraints of Sch TF-20 and Pall 442T candle filters are illustrated in Figures 2. Nine experimental data sets corresponding to 9 different candle filters are shown. Each line represents a nondimensional Young's modulus (α) obtained by the FEM model of the candle filter. Figure 2a shows the boundary restraint effects on the second bending mode. Figure 2b shows the boundary restraint effects on the third bending mode. The experimental frequency results of each filter together with its K value, which can be obtained following Kiriakidis and Chen (2002), are plotted in both bending modes. The symbol that appears close to the α lines represents the candle filter's material properties. Linear interpolation is used to get the α values for the candle filters that reside in between lines. The values of α at different boundary restraints (K values) must be the same in both the second and the third bending modes. Using this figure, the Young's modulus and the boundary restraint of each candle filter are determined simultaneously.

Thermal dynamic characteristics

The natural frequencies and mode shapes obtained from the thermal dynamic testing are presented along with those from the finite element analysis. Room, 250°F and 350°F

temperatures are used to test 2 new Sch TF20 and 2 Pall 326 filters. Of these 4 filters tested, the results of one filter of each type are shown. The results of the other two filters are similar to those presented.

Table 1 lists the natural frequencies of the Sch TF20 335i-173 filter at different temperatures with free-free boundary conditions. At 250°F the natural frequency values dropped about 1.6% and at 350°F they decreased about 3.8%. The frequency shift can be due to a reduction of Young's modulus and/or change in the filters dimension (thermal expansion). When comparing the frequency ratio of two consecutive frequencies, the values are approximately the same at all three temperatures. This result indicates that there is no change in the setup boundary restraint. The natural frequencies with fixed-free boundary conditions are also listed in this table. Again, there is a clear reduction of the natural frequencies with temperature increments. There is about 1.4% and 3.0% reduction at 250°F and 350°F, respectively. The frequency ratios of second and third vibration modes decrease at elevated temperature. Therefore the boundary restrain K^ increases with the increment of temperature. The nondimensional K^ factor are 2.75 for room temperature, 2.82 for 250°F, and 3.0 for 350°F.

Table 2 lists the thermal result for the Pall 326 1365-5 filter. Similar thermal behavior is observed in this filter. The percentage reduction in the frequency results is about 1.6% for 250°F and about 2.2% for 350°F. In the free-free test, the elevated temperature effect on the boundary restraint is minimal. With the fixed-free boundary restraints, there is a reduction of about 0.8% and 2.6%, respectively. The frequency ratio f3/f2 decreases with the increment of temperature. The nondimensional K^ factors are 10.45 for room temperature, 10.6 for 250°F, and 11.15 for 350°F.

Transient thermal analysis using a 3-D FEM model was conducted to evaluate the temperature distribution in the candle filter during back-pulse cleaning. The filter was assumed to have 1500°F uniform temperature before back-pulse and the back-pulse has a constant temperature of 77°F with 0.5 sec duration. Figure 3 shows the temperature distribution along the thickness of the Pall 326-filter model with respect to time. During the first 0.5 seconds the temperature decreases fast in a concave way. After the thermal load is removed the fitter's temperature increases. It takes about 2 extra seconds for the filter to reach back to the steady state temperature condition of 1500°F. The maximum temperature difference occurs at the surface of the inner wall at 0.5 seconds. The temperature between 0.215in and 0.304in from the inner wall reaches its minimum temperature at about 0.6 second. Alvin (1999) reported experimental thermal transient event occurred during back pulse cleaning. The experimental temperature drop observed during back pulse and the current FEM simulation results are similar. For the Sch TF20 filter, the maximum temperature difference also occurs at the inner wall at 0.5sec. After 2.5 seconds, the filter goes back to 1500°F uniform temperatures.

The nodal temperature distribution obtained at different times is used as nodal thermal loading input for the FEM stress analysis. Linear stress analysis is performed on both filter models to obtain the maximum principal stresses. The stress distributions along the wall of the Pall 326 model at 0.5sec, 0.55sec, 0.60sec and 0.65sec time periods are plotted in Figure 4. The maximum stress (about 2055psi - tension) is found in the inner wall at 0.5sec. A maximum stress of about 919psi is noticed at 0.15in from the inner wall at 0.55sec. Between 0.22in and 0.3in from the inner wall the maximum stress values happen at 0.6sec and 0.65sec. These stresses are about 570psi and 201psi, respectively. The outer walls of the filter models have no stress because there is no change in the surface temperature. For the Sch TF-20 model, the

maximum stress is also found in the inner wall at 0.5sec and is about 1346psi (tension). The maximum stress found at 0.15in, 0.22in, and 0.3in from the inner wall are about 624psi (0.55sec), 396psi (0.60sec), and 138psi (0.65sec), respectively. The thermal stress values obtained using FEM are quite significant when compared with the as-manufactured material strength of the Pall 442T and Sch TF-20 filters. These stresses have been obtained assuming constant back pulse temperatures of 77°F. The actual back pulse temperature applied to the candle filters may be higher than 77°F because the back pulse gas might travel through a number of hot pipes inside the plenum. Therefore the maximum thermal stresses that the filters will be subjected to can be lower than the assumed 77°F back pulse.

Fatigue

The vibration of the candle filter, due to plenum shaking and back-pulse cleaning, needs to be considered. In the first phase of this fatigue analysis, the natural frequency and damping ratio are determined experimentally using the frequency response curve. The shaker is operated at a selected frequency, the candle filter response is observed while the transient part damps out, and the amplitude of the steady state is recorded during different shaking frequency. For example, the shaking frequency used to excite the Sch TF20 326I-147 filter ranges from 8Hz to 14Hz. Using the RAM curve the first natural frequency is consistent with that obtained using the impact excitation test. The damping ratio is also obtained from the RAM, using the half power points method. The first natural frequency for the Sch TF20 335i-159, 379H-129, and 335I-173 filters are about 10Hz, 10.2Hz, and 8Hz, respectively. The damping ratios are about 0.014, 0.041, and 0.048, respectively.

These four candle filters are used to build the fatigue life curve for the Schumacher TF20 filters. The maximum amplitude of the ground acceleration used to excite the Sch 326I-147, 335I-159, 379H-129, and 335I-173 filters are about 0.27g, 0.31g, 1.85g, and 0.65g, respectively. The shaking frequencies used were 9.75Hz, 9.75Hz, 10Hz and 7.5Hz, respectively. Therefore the maximum bending stresses obtained at the base of these filters are about 938psi for the 326I-147 filter, 994psi for the 335I-159 filter, 884psi for the 379H-129 filter, and 1036psi for the 335I-173 filter. Figure 5 shows S/N curve for the Sch TF-20 filters. With this curve, the number of cycles that the Sch filters can go through before failure is determined. It is noticed that when the filters are subjected to stress about 1036psi, the number of fatigue cycles needed to cause a catastrophic failure is about 8,100 cycles. If the stress is reduced to about 884psi, the number of cycles increases dramatically (about 4,906,650 cycles).

Reliability

The probability of failure function obtained using the Weibull hazard function (Mann et al. 1974) is given by

$$P_T(t) = 1 - L^i_T(t) = 1 - \exp\left[-\int_0^t h^i_T(x)\,dx \right] = 1 - \exp\left[-\left(\frac{x-\lambda}{\eta} \right)^{\beta} \right] \qquad (1)$$

The function $h_T(t)$ is called hazard function and L^i_T is the reliability function. $h_T(t)$ is introduced because certain general characteristics of the performance of systems subjected to repeat loads are easily studied by the behavior of their hazard functions. The hazard rate for the

Weibull distribution is decreasing in x-λ if β <1 (or increasing when β>1), and is independent of x if β=1. When β=1 the Weibull distribution specializes to the exponential distribution. β is known as the shape parameter and λ is the location parameter.

Consider the case where the only parameter that affects the deterioration of the filters is the exposure time and that all other factors are constants. A simplified hazard function of the Schumacher TF-20 filters can be assumed as

$$\int_0^t h^i{}_T(x)\,dx = \left(a + b\left(\frac{E_0 - E_t}{E_0} \right) \right)^{\beta} \tag{2}$$

where a and b are distribution parameters that are obtained experimentally. E_0 is the Young's modulus of the filter in the new stage and E_t is the Young's modulus after t exposure hours. For this particular ceramic candle filter group the value of the shape parameter β is assumed to be 3.6. The parameters a and b obtained experimentally for the median curve are about 0.017and 0.123, respectively. The maximum exposure hours assumed in this equation is 2650hr which is the maximum time that the Sch TF-20 candle filters tested during this study had been exposed. It is assumed that the maximum allowable damage at 2650 exposure hours is about 12.9%. If candle filters with more exposure hours are included, new values for the distribution parameters will need to be recalculated.

The probability of failure equation can be now formulated by using Equation (1) and (2) as

$$P_T(t) = 1 - \exp\left(-\left[a + b\left(\frac{E_0 - E_t}{E_0} \right) \right]^{\beta} \right) \tag{3}$$

Figure 6 shows the serviceability curve for the Sch TF-20 filters. The filters that reside on the left-hand side of the "median curve" are considered safe. The filters that are in between the media curve and the "upper-band curve" needs a close structural property evaluation and the filters that fall on the right-hand side of the "upper-band curve," away from the curve are considered unsafe. Consider the 324 H07 Sch TF-20 filter, which has been tested at 500-hr and 2650-hrs. The Young's modulus reductions of this filter are 4.8% and 10.19% respectively. Using Figure 6 it is noticed that the filter is in the safe region at both exposure times. This result could be empirically confirmed if the stiffness reduction of this filter is compared with the behavior of other filters with the same exposure hours. The reliability of this filter at 500hrs is about 0.8 (probability of failure 20%) and after 2650hrs the reliability is about 0.18, which means that even though this filter has been used for about 2650hrs, it can still be used but close attention must be paid to the filter's material properties.

Conclusions

Results from this study indicated that dynamic characterization is a feasible NDE technique for studying structural properties of ceramic candle filters. It has been shown that the degradation of the filters due to long working could be reflected from the shift of natural vibration frequencies. These shifts are due to changes in structural properties such as stiffness, which are directly related to the Young's modulus of the candle filters. A technique that uses the

frequency ratios of the second and the third vibration bending modes to evaluate the boundary restraints of the candle filters was developed. The boundary restraints and Young's modulus of a candle filter can be predicted simultaneously using this technique. A combination of mode shape and strain energy analysis worked successfully in detecting damage zone along the filter span. The vibration signature can be also used to evaluate the stiffness and boundary restraints of the ceramic candle filters at elevated temperatures. A relationship between the stiffness reduction and the reliability of the ceramic candle filters due to exposure hours has been presented. Fatigue results from the present study show the importance of considering the operational vibration as well as temperature gradient as factors that may also produce failure in the ceramic candle filters. Further studies are recommended in implementing the dynamic NDE characterization methods for actual in-situ conditions, and in establishing a systematic testing procedure for field applications.

Applications and Future Activities

Attractive features of the proposed NDE method include low cost, ease of operation, nondestructive nature, and adequate sensitivity to identify stiffness degradation in the filters. Using the techniques developed in this study to determine the degradation and the remaining life of the ceramic candle filters can lead to a more efficient power generation process, avoiding unexpected shut downs due to candle filter failures.

Further studies are suggested to investigate the in-situ operational variations, and to establish a systematic testing procedure for field application. Even though several important parameters have been studied during this research for the remaining life prediction of the ceramic candle filter, the actual in-situ environments may present many important physical effects needed to be considered further. For example, fatigue and large amplitude shaking due to plenum vibration and back-pulse shaking, thermal attack due to back pulse temperature-drop, the pressure-level history and the temperature history in the plenum and the possible chemical attack due to various coals. The actual operating history of the candle filter is the key aspect for the prediction of the remaining life. The above physical effects need to be included in the description of the operating history. The exposure hours that have been reported by the power plant are only one aspect of the actual history of the filter. Further development of an in-situ remaining life prediction of the candle filter system is proposed to consider the detailed operation history of the candle filters.

Acknowledgment

The authors acknowledge the support from the National Energy Technology Laboratory (NETL), Department of Energy, for this study under the contract DE-FG26-99FT40202. Special thanks are extended to Ted McMahon of NETL/DOE for his valuable comments and technical support through out this study. The authors also acknowledge the help from Richard Dennis of NETL /DOE and Howard Hendrix of Southern Company Services for his help in providing the filter specimens.

References

Alvin, M. A., Tressler, R. E., Lippert, T. E., and Diaz, E. S., 1994. "Durability of Ceramic Filters." Advances in IGCC and PFBC Review Meeting, DOE/METC-94/1008, Vol 2, DE94012252, 545-571.

Alvin, M.A., 1999. "Hot Gas Filter Development and Performance." High temperature Gas Cleaning, Institut für Mechanische Verfahrenstechnik und Mechanik Universität Karlsruhe – Germany-1999, Vol. 2, 455-467.

Chen, H.L. and Kiriakidis, A., 2000. “Stiffness Evaluation and Damage Detection of Ceramic Candle Filters.” *Journal of Engineering Mechanics* 126(3): 308-319.

Chen, H.L. and Kiriakidis, A., 2001. “Evaluation Structural Properties of New Ceramic Candle Filters Using Dynamic Characterization Method.” *Material Evaluation*, 59(1): 63-69.

Kiriakidis, A. and Chen, H. L., 2002. “Implementation and Application of NDE on Ceramic Candle Filters.” Final Report No DE-FG26-99FT40202 to FETC/DOE, Morgantown, WV.

Lippert,T. E., Bruck, G. J., Sanjana, Z. N., and Newby, R. A. 1994. “Westinhouse Advanced Particle Filter System.” Advances in IGCC and PFBC Review Meeting, DOE/METC-94/1008, Vol 2, DOE94012252, 535-544.

Mann, N. R., Schafer, R.E., and Singpurwalla, N. D., 1974. “Methods for Statistical Analysis of Reliability and Life Data.” John Wiley & Sons, New York.

Pontius, D. H. and Starrett, H. S., 1994. "Properties of Ceramic Candle Filters." Proceeding of the Coal-Fired Power System 94, DOE/METC-94/1008, Vol.2, DE94012252, 572-574.

Spain, J. D. and Starrett, H. S., 1999. “ Characterization of Monolithic and Composite Filter Elements." High temperature Gas Cleaning - Institut für Mechanische Verfahrenstechnik und Mechanik Universität Karlsruhe – Germany 1999, Vol. 2, 414-427.

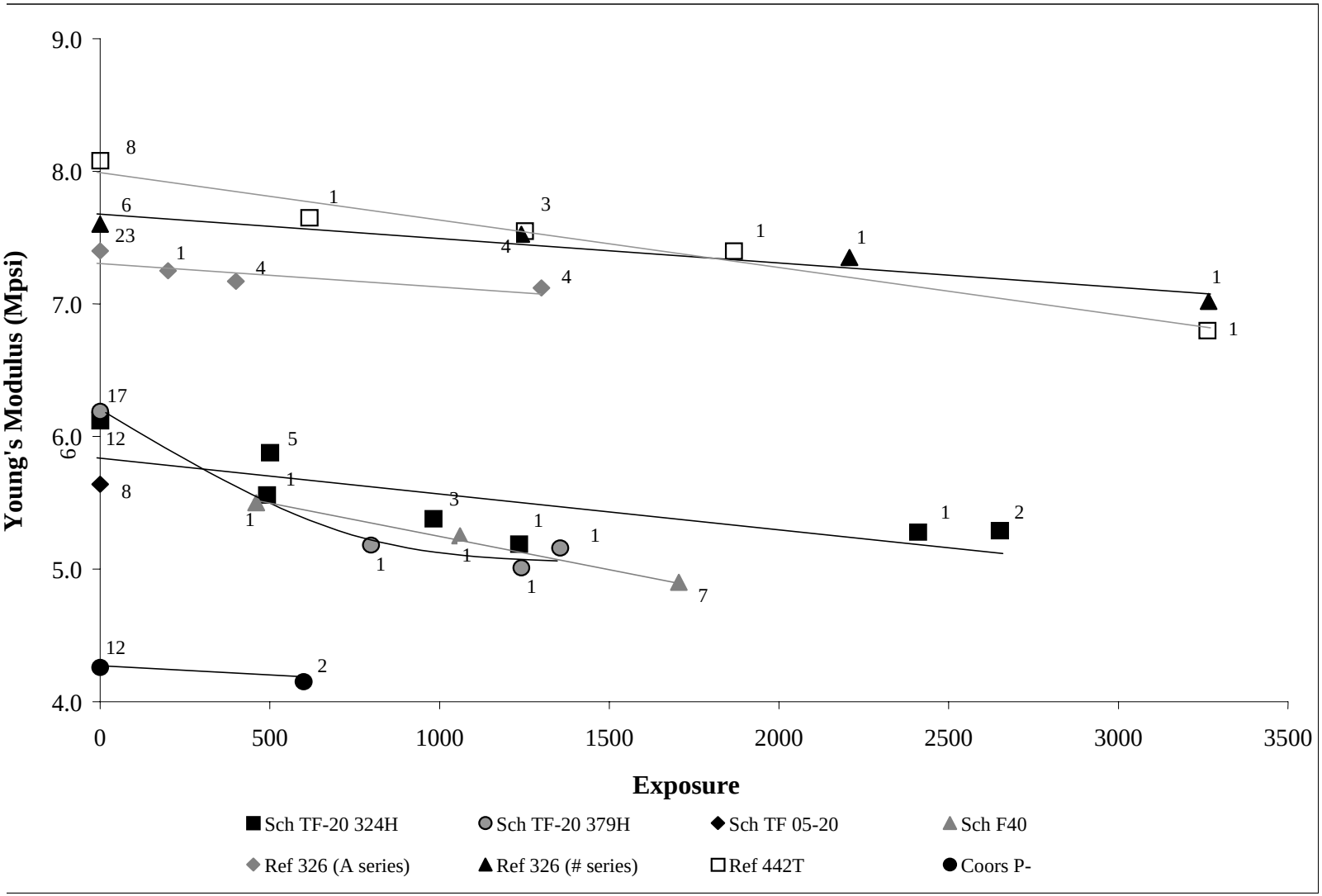

Figure 1 Average Young's modulus deterioration of ceramic candle filters at different exposure hours

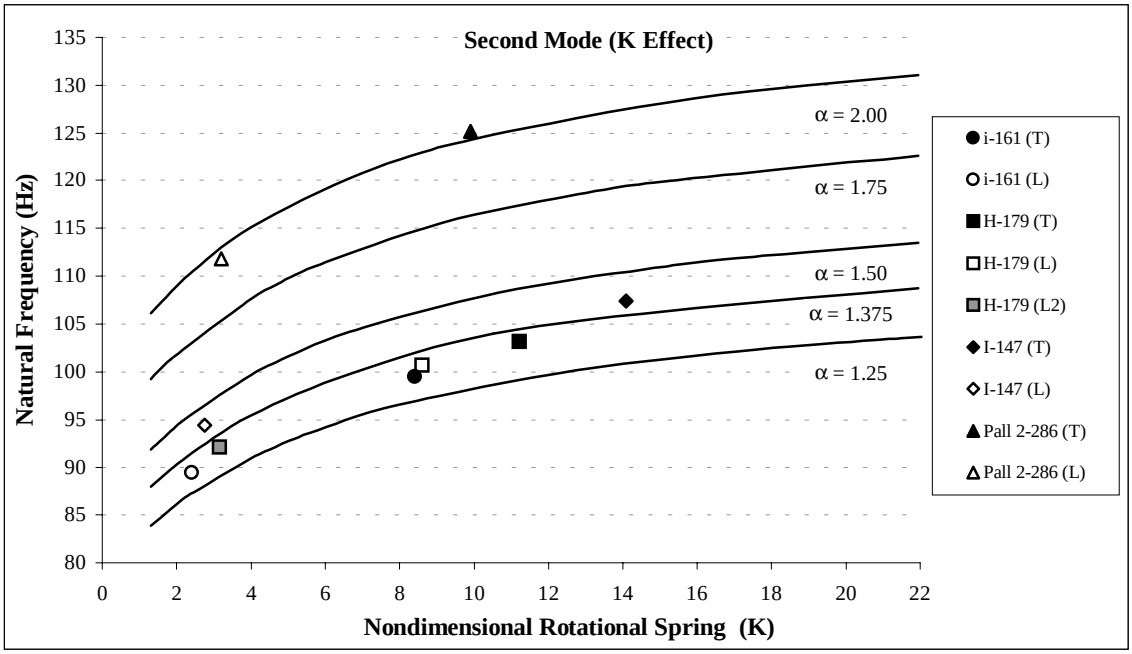

Figure 2a Nondimensional stiffness K effect on the second mode of Sch TF-20 and Pall 442T filters

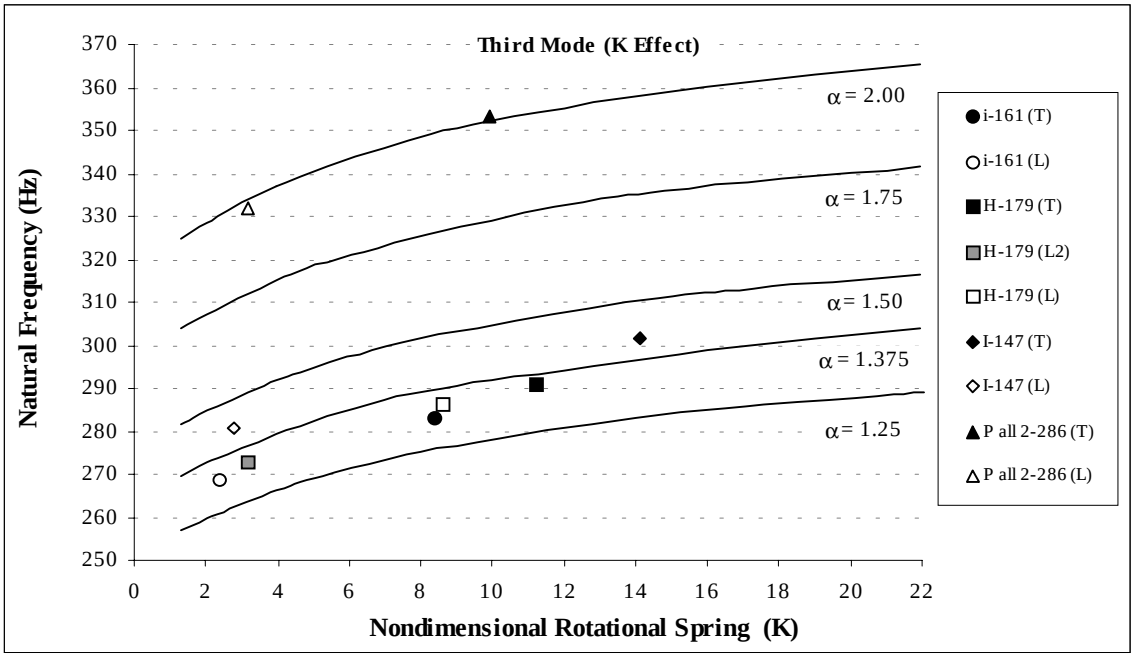

Figure 2b Nondimensional stiffness K effect on the third mode of Sch TF-20 and Pall 442T filters

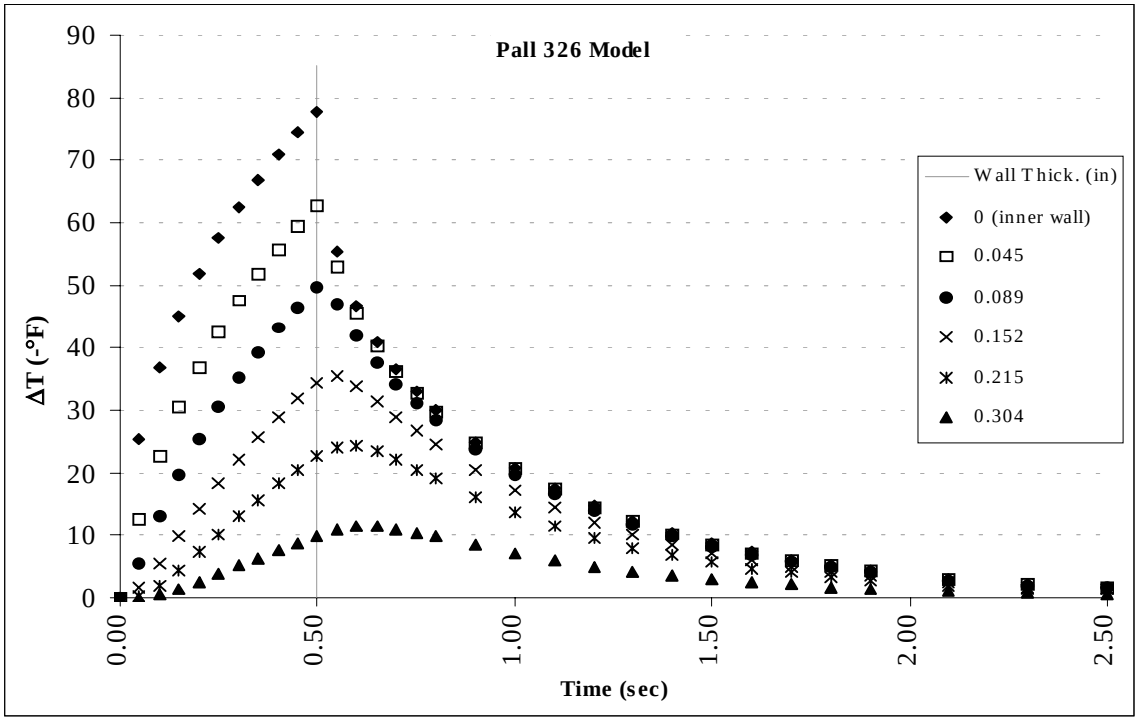

Figure 3 Temperature distribution time history along the thickness

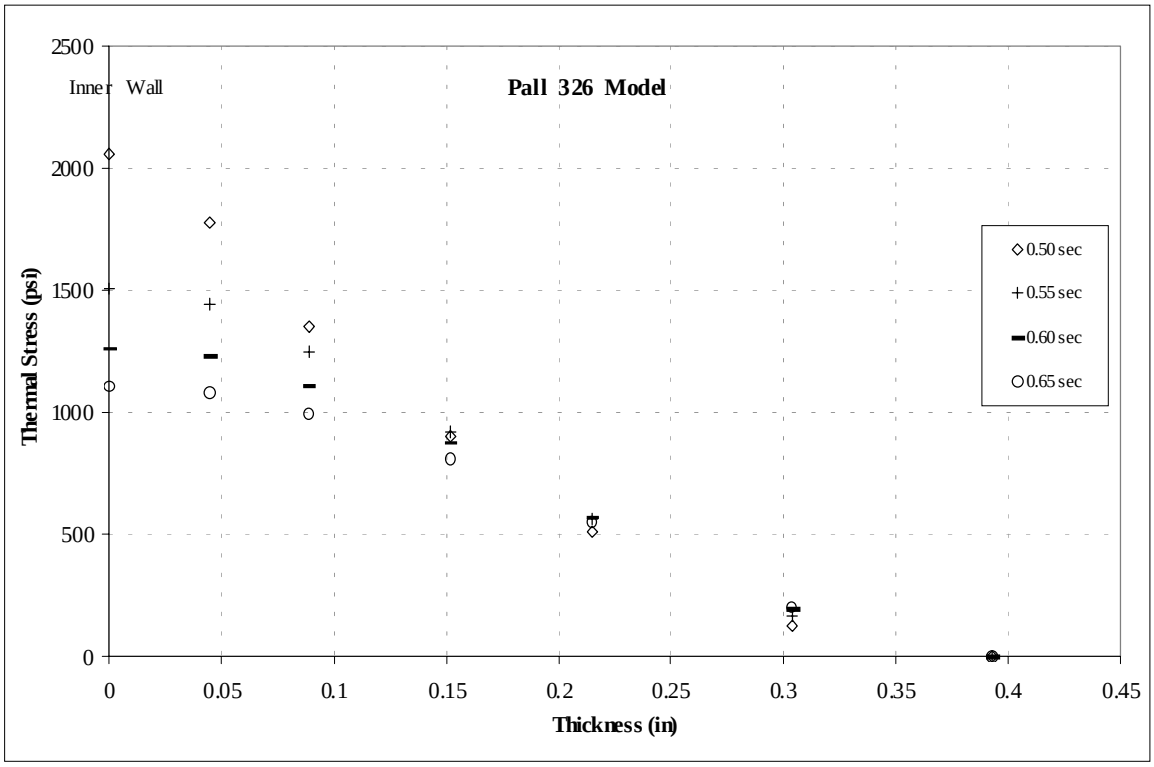

Figure 4 Stress distribution along the thickness

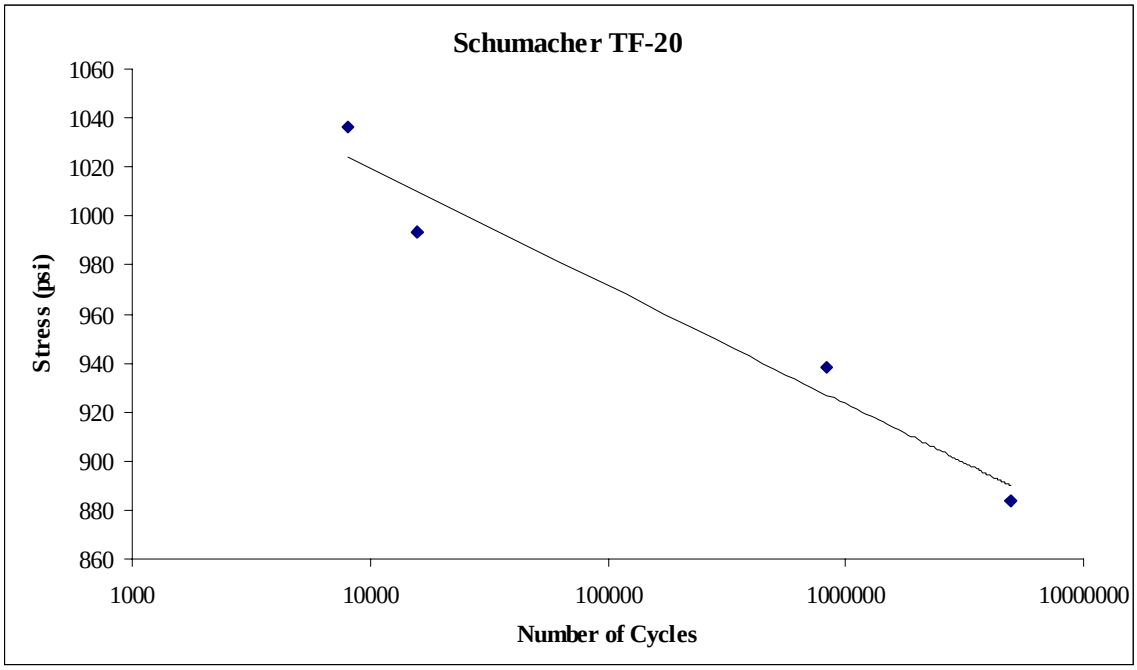

Figure 5 Fatigue life curve for two Sch TF-20 filters

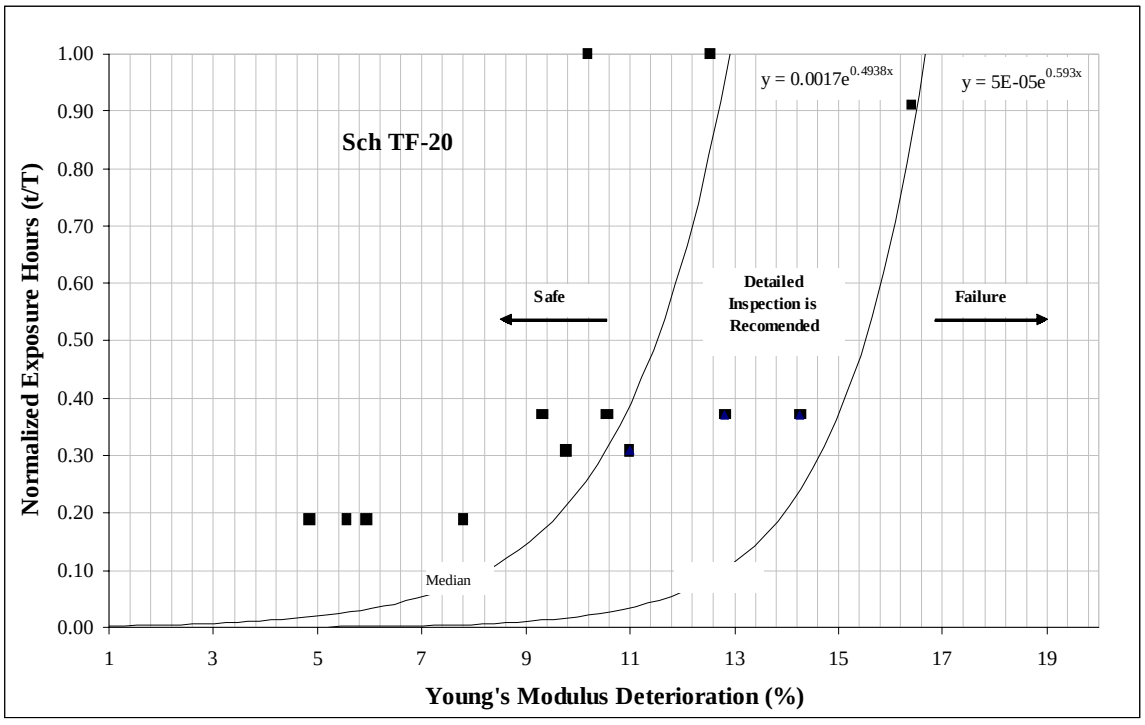

Figure 6 Percentage deterioration of Sch TF-20 filters with respect to exposure hours

Table 1 Natural frequencies (Hertz) of a Sch TF20 filter at different temperatures

Schumacher TF-20 3-351-173					
FREE-FREE BC					
Mode	**Room**	**250°F**	%	**350°F**	%
1	115.36	113.53	1.613	111.08	3.846
2	314.94	310.06	1.575	303.34	3.823
3	610.46	600.59	1.644	587.77	3.861
4	993.04	976.56	1.687	956.03	3.871
5	1452.64	1429.44	1.623	1401.20	3.671
6	1974.49	1948.96	1.310	1909.28	3.415
FIXED-FREE BC					
Mode	**Room**	**250°F**	%	**350°F**	%
1	18.31	--	--	--	--
2	111.39	109.86	1.389	108.14	3.007
3	331.22	326.54	1.433	320.43	3.365

Table 2 Natural frequencies (Hertz) of a Pall 326 filter at different temperatures

Refractron 326 1365-5					
FREE-FREE BC					
Mode	**Room**	**250°F**	%	**350°F**	%
1	137.33	135.80	1.124	134.28	2.273
2	375.84	369.26	1.781	367.74	2.204
3	724.19	711.46	1.790	708.41	2.228
4	1170.35	1152.04	1.589	1145.94	2.130
5	1702.88	1675.42	1.639	1666.26	2.198
6	2311.45	2278.13	1.463	2264.40	2.078
FIXED-FREE BC					
Mode	**Room**	**250°F**	%	**350°F**	%
1	18.31	--	--	--	--
2	123.60	122.57	0.837	120.54	2.532
3	349.43	346.37	0.881	340.27	2.691